Tea derived carbon dots with two ratiometric fluorescence channels for independent detection of Hg^{2+} and H_2O

Chuanlu Ding[a], Hao Xing[a], Xuhong Guo[a,b], Huihui Yuan[c], Cuihua Li*[,a], Xiulan Zhang*[,a], Xin Jia*[,a]

[a] School of Chemistry and Chemical Engineering/Key Laboratory for Green Processing of Chemical Engineering of Xinjiang Bingtuan, Key Laboratory of Materials-Oriented Chemical Engineering of Xinjiang Uygur Autonomous Region, Engineering Research Center of Materials-Oriented Chemical Engineering of Xinjiang Bingtuan, Shihezi University, Shihezi 832003, People's Republic of China

[b] State Key Laboratory of Chemical Engineering, East China University of Science and Technology, Shanghai 200237, People's Republic of China

[c] Shanghai Key Laboratory of Functional Materials Chemistry, School of Chemistry & Molecular Engineering, East China University of Science and Technology, Shanghai 200237, China

E-mail: xl_zhang@shzu.edu.cn (X. Zhang); jiaxin@shzu.edu.cn (X. Jia); lich@shzu.edu.cn (C. Li)

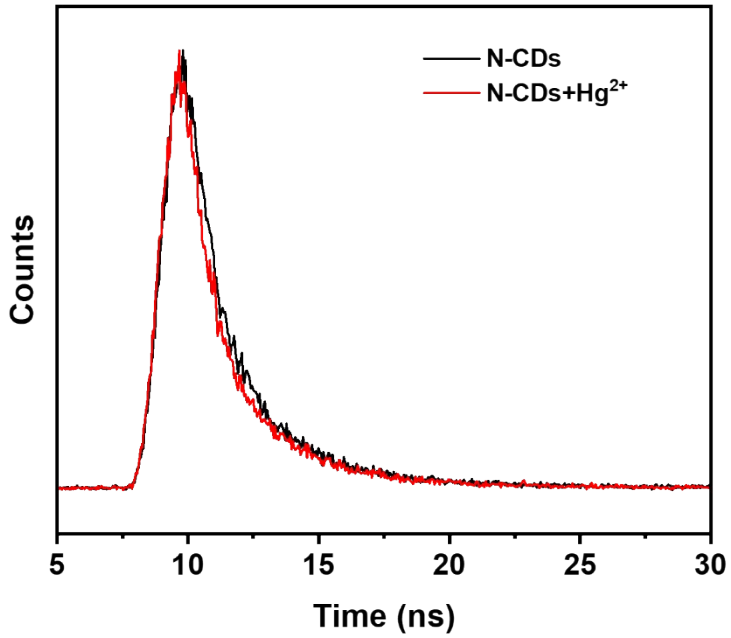

Fig. S1 Time-resolved fluorescence decay curve of N-CDs and N-CDs+Hg^{2+}.

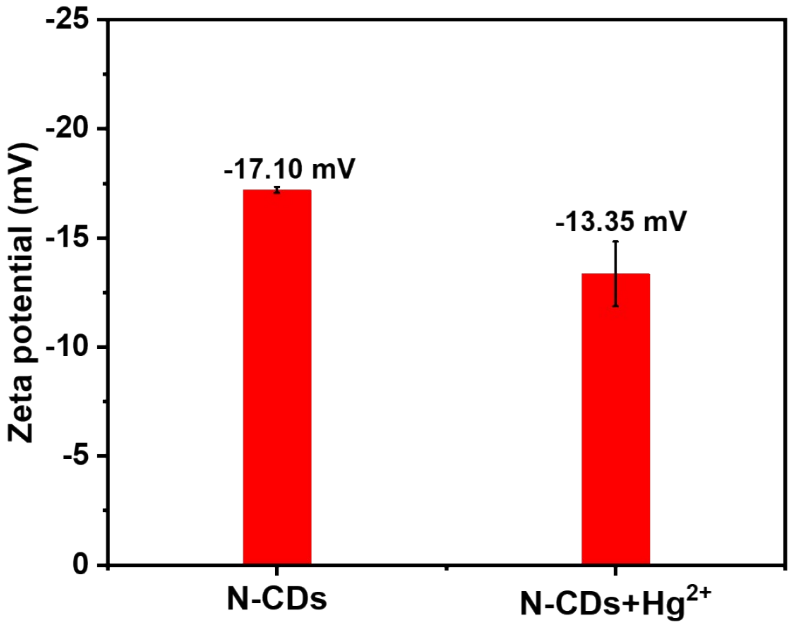

Fig. S2 Zeta potential value of N-CDs and N-CDs+Hg^{2+}.

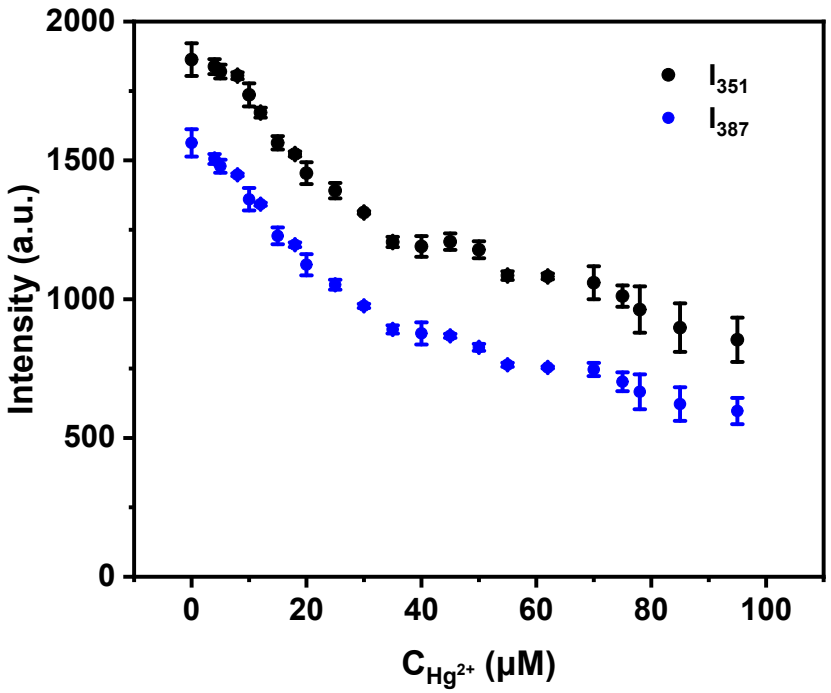

Fig. S3 I_{351} and I_{387} value of N-CDs changes with concentrations of Hg^{2+}.

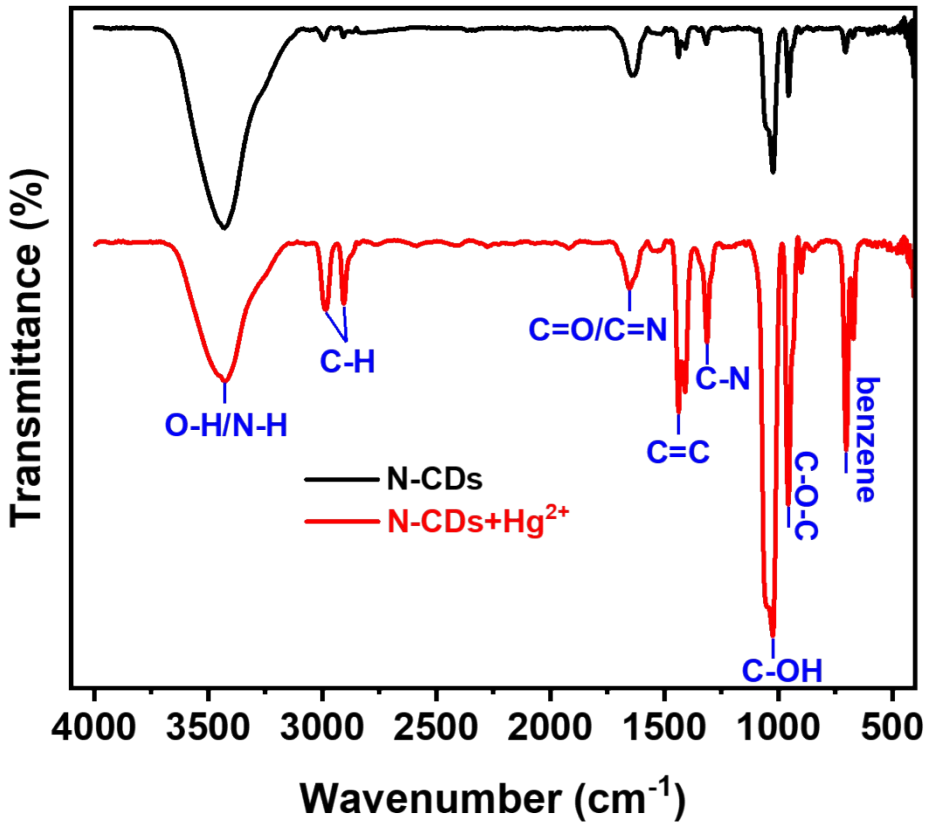

Fig. S4 FTIR spectra of N-CDs and N-CDs+Hg^{2+}.

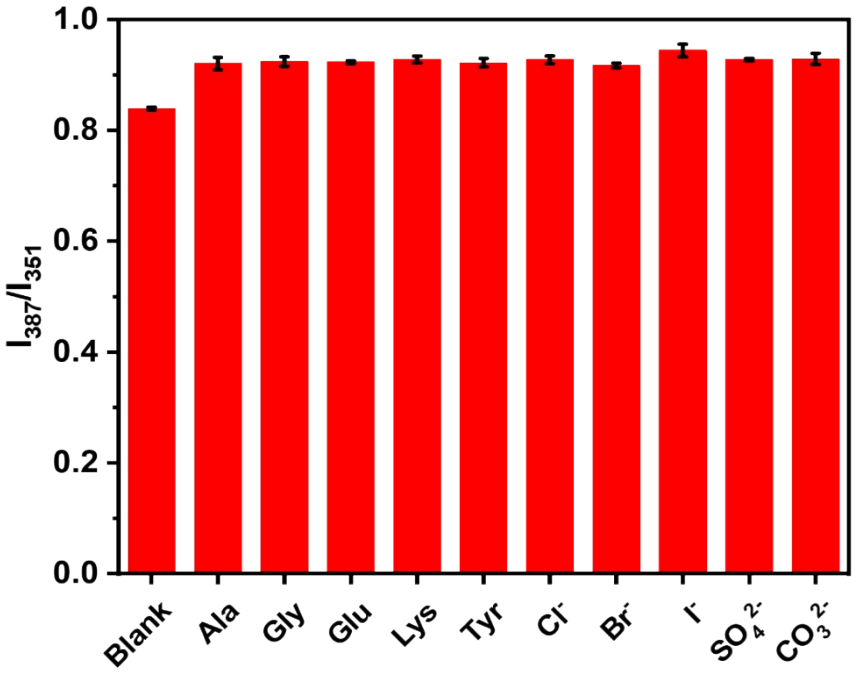

Fig. S5 I_{387}/I_{351} values for interference ions (50 μM) mixture with N-CDs.

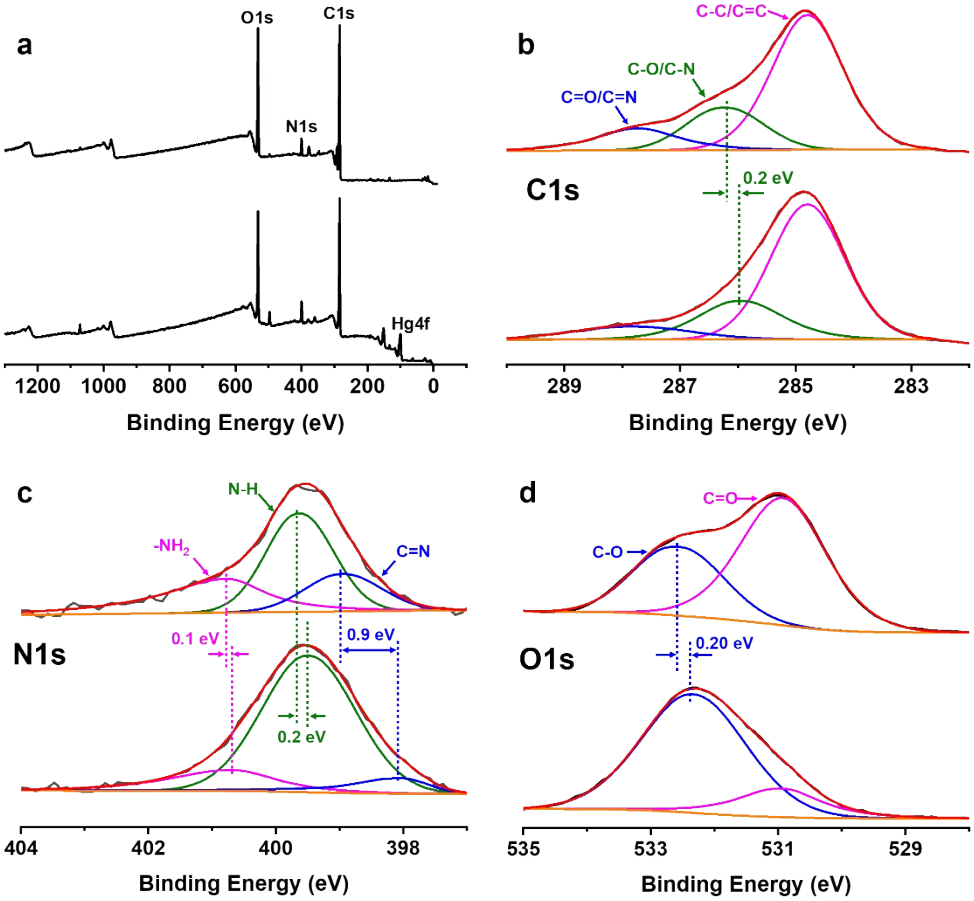

Fig. S6 (a) XPS spectra, (b) XPS C1s spectra, (c) XPS N1s spectra, (d) XPS O1s spectra of N-CDs (upper spectra) and N-CDs+Hg^{2+} (nether spectra).

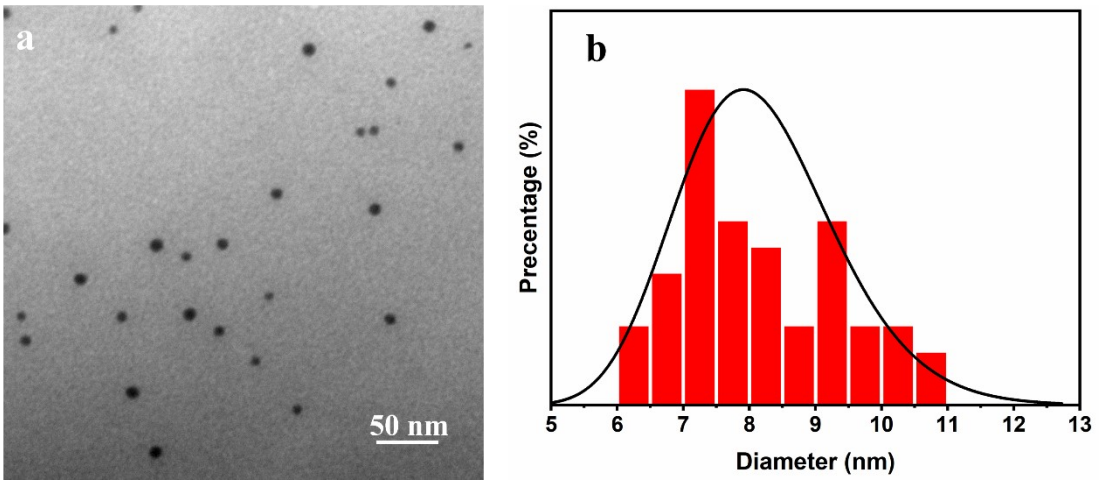

Fig. S7 (a) TEM image, (b) Particle size distribution analysis of N-CDs+Hg^{2+}.

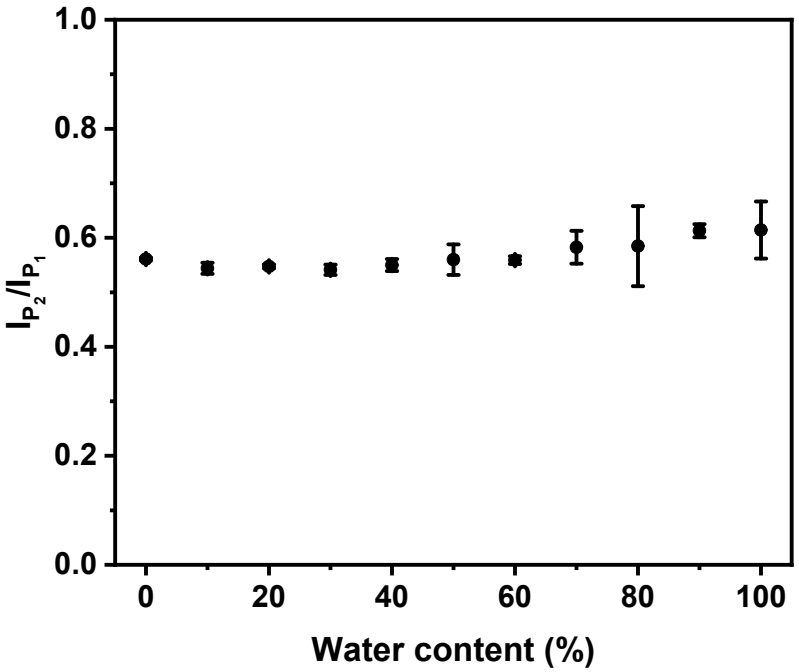

Fig. S8 Plot of I_{P2}/I_{P1} versus the water content in ethanol, where P2 and P1 is the fluorescence emission peak around 387 nm and 351 nm, respectively.